Supplement for

"Cell growth model with stochastic gene expression helps understand the growth advantage of metabolic exchange and auxotrophy"

Dibyendu Dutta, Supreet Saini

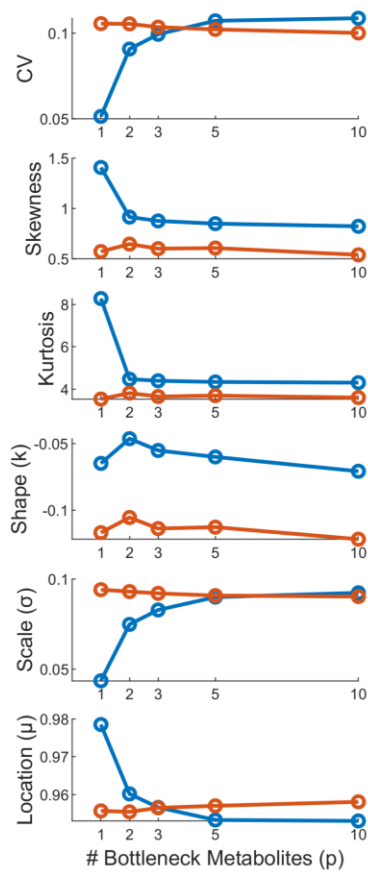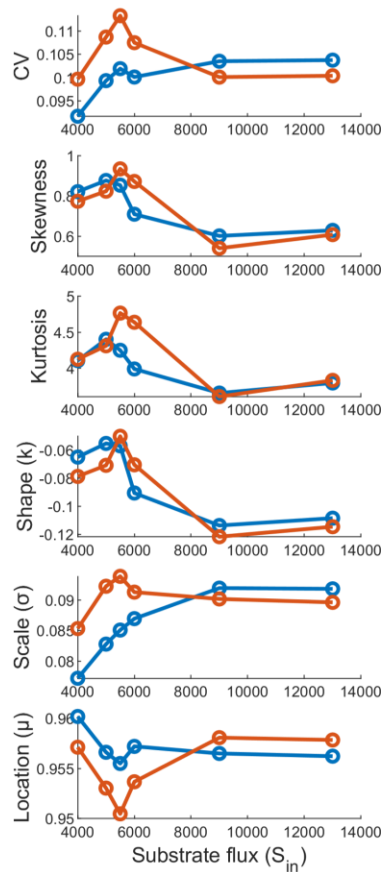# Contents

S1. Analysis of Distributions of generation times obtained from simulation

Here we plot the Coefficient of Variation (CV), Skewness, Kurtosis, for the distributions of generation times obtained in various simulated conditions.

We also plot the log GEV fit parameters – Shape (k), Location (μ), Scale (σ).

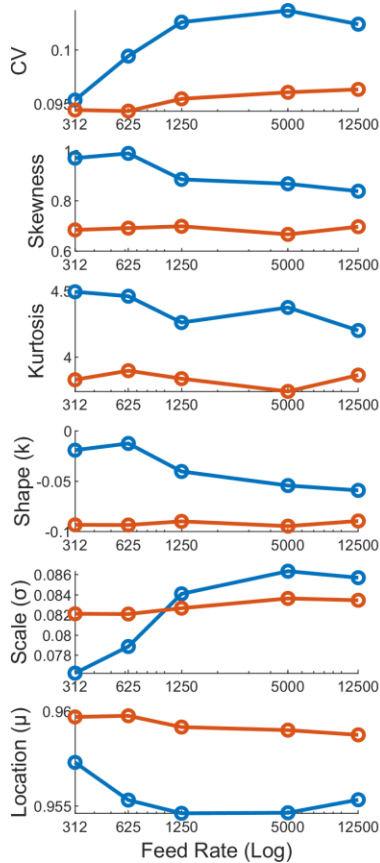**Figure S1: Variation of CV, Skewness, Kurtosis, and the log GEV Fit parameters for distributions of generation times across different conditions**

(a) Varying p (Fig 2b), Low Sin (blue), high Sin (red).
(b) Varying Sin (Fig 2c), blue – p=3, red – p = 10.
(c) Varying metabolite import/feed rate (Fig 3a and 3b), low Sin (blue), high Sin (red).
(d) Varying metabolite secretion ratio (Fig 3e and 3f), low Sin (blue), high Sin (red).
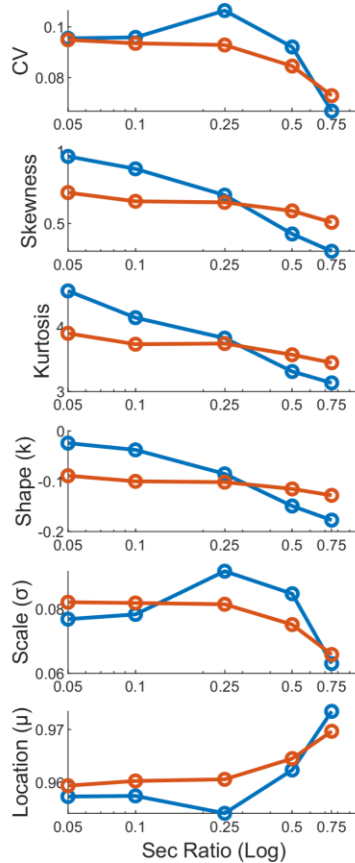
S2. Analysis of experimentally observed single cell growth of *E. coli* in different media conditions (Dataset from Taher-Araghi *et al.* Curr Biol 2015)

Growth of E. coli at a single cell resolution at various media conditions was studied using microfluidic device called Mother machine, in (1).

They measured the growth of E. coli in the following media conditions: Tryptone Soya Broth (TSB), Synthetic Rich media, glucose, glucose+6aa, glucose+12aa, sorbitol, and glycerol.

We analysed the dataset to obtain the cell doubling times and plotted the distributions. We fit the distributions to both Generalized Extreme Value distributions (Fig – S2a) and Log-Generalized Extreme Value distributions (Fig – S2b).

In order to compare the fit of the data between these two distributions, we sampled 1e6 random data points from the fit distributions of the two types, and then ran a two sampled Kolmogorov-Smirnov test, with the original dataset and the sampled random data from the two distributions, and found the test was unable to reject the null hypothesis that both datasets are from the same distribution, even at 1e−8% significance level! Thus, from our analysis we find both types of distributions (GEV and log-GEV) with appropriate parameters can fit the bacterial cell generation time distributions well.

We plot the fit parameters of the GEV distribution and log-GEV distribution across different media conditions from the dataset in Figure – S2c and S2d respectively. We find that the fit value of the shape parameter (k) < 0, across all the conditions in the dataset. Thus, our analysis finds the distributions fit best by the Reverse Weibull (GEV Type III) and log-Reverse Weibull, and not by log- Fréchet (GEV Type II, k > 0) as found by previous analysis (2). The difference in our results could stem from the fact that the dataset we analyse is different. Additionally, the magnitude of fit value of shape parameter is very low (GEV: -0.07 to -0.02 and log GEV: -0.15 to -0.05), thus the nature of the shape is not too different from Fréchet with shape parameter k > 0.

We also analysed the dataset to obtain its mean generation time, the coefficient of variance (CV), skewness and kurtosis (Fig – S2e). The dataset shows that the CV of the experimentally obtained distribution ranges from about 6–14%.
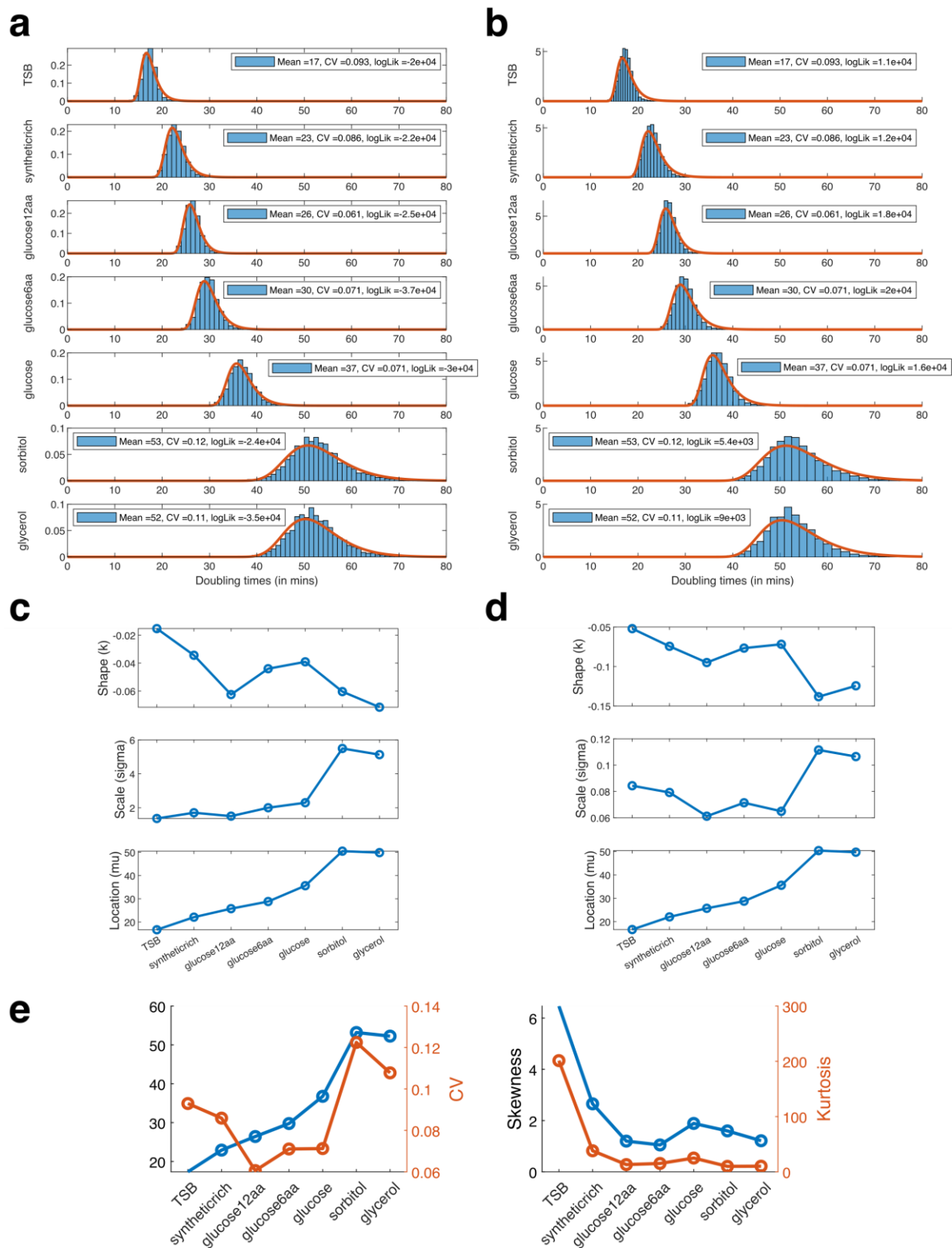
Figure S2: Analysis of the Taher-Araghi 2015 dataset

(a) Fit of the dataset to GEV distribution. (b) Fit of the dataset to log-GEV distribution. Fitted parameters of (c) GEV distribution, (d) log-GEV distribution, for each of the different media conditions in the dataset arranged in ascending order of mean generation time.

S3. Shape of the distribution of bacterial doubling times from our model

We started our model using the original parameters of t_{ON} and t_{OFF} from Golding et al. 2005, which led us to generation time distributions that had too high a Coefficient of Variation (CV ~ 0.45), when we chose a metabolite threshold value that yielded physiological mean generation times ~30-50 mins. (Fig – S3a).

Upon varying the metabolite threshold, we found that we could obtain the requisite range for the CV, but using a much higher value for the threshold (Fig – S3b), which also results in a much greater mean generation time (Fig – S3b). Moreover, the shape of the distribution also changes greatly due to the variation of the metabolite threshold parameter (Fig – S3c). However, the change in shape is reminiscent of how the shape of the GEV distribution changes as its parameters change.

Within the framework of our simplistic model, the above observation suggests that the noise profile of growth-determining biosynthetic metabolic enzymes in a bacterial cell is much lower than the noise profile of a synthetic promoter whose expression characteristics was measured in Golding et al. 2005 (3). We, hence searched the parameter space of the t_{ON}, t_{OFF}, and threshold parameters to find the values at which we can find physiological values of mean generation time as well as the CV (Fig – S3d–S3g). We finally chose: $t_{OFF} = 2.4$ min, $t_{ON} = 4$ min, Threshold = 1e7.

Additional factors that affect cell generation time distribution

1. **DNA Replication**

Our model captures the dynamics of metabolite accumulation due to stochastic gene expression, and its effect on growth. As cell grows, more proteins are made but cell size also increases, thus protein concentrations that determine the probability of burst frequencies remain unaltered. However, DNA replication also takes place during growth, which could potentially double the rate of gene expression, if not limited by the transcription machinery. In case replication increases gene expression, protein number and metabolite production also should increase, which in turn may allow the slow pathways to produce more and reach the requirement threshold earlier and hence

decrease the generation times. Thus, with DNA replication incorporated, we expect the generation time distributions may reduce its width (CV) for the same set of gene expression parameter used in the model.

2. Cell size variations

Our model assumes strict metabolite level sizer and adder laws for division, which can be thought of as a proxy for cell size. In our model we have considered both perfect partition between the cells as well as imperfect partitioning (Supplementary S6), and find little difference between the nature of the outcomes. Previous models have also claimed that it is not possible to distinguish between the nature of noises from gene expression and imperfect partitioning (4).

Further in case, there is a noise in terms of the cell's size perception to trigger division, it is likely to only add an extra short delay on to the result. Additionally, experiments have shown that cells seems to follow the size law when growing in poorer media at slower rates, and follow the adder when growing faster in richer media (5). We do not understand how such changes alter the generation time distribution.
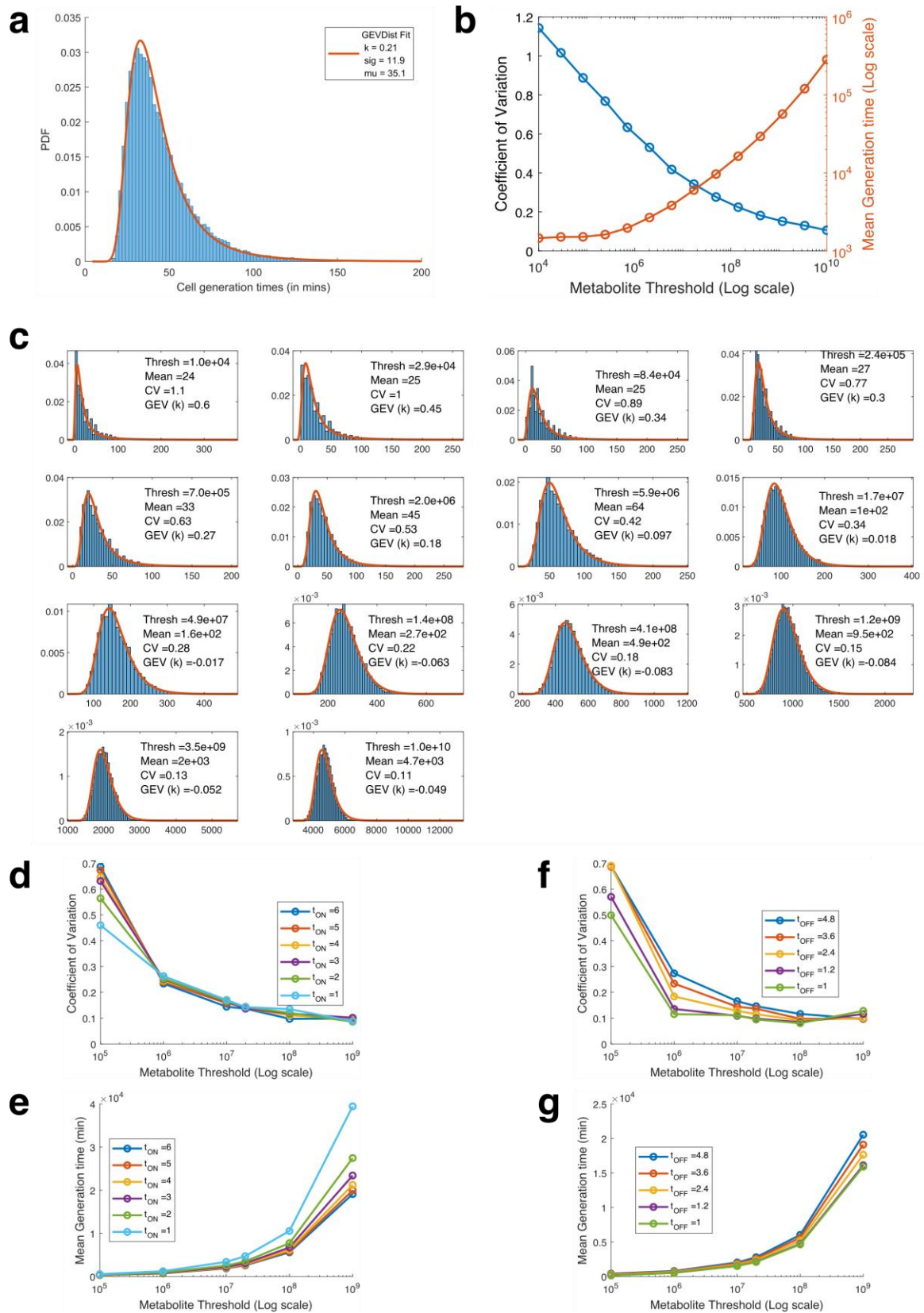
Figure – S3: Shape of the distribution of bacterial doubling times from our model
(a) Generation time distribution with Golding parameters. Change in (b) CV and mean generation time, (c) Shape of distribution, with metabolite threshold. Change in CV (d,f) and mean generation time (e,g), with changing metabolite threshold, and varying gene expression parameters: tON (d,e), tOFF (f,g).

S4. Metabolic Adder and Metabolic Sizer Models

Our framework connects stochastic gene expression with growth by transforming the cell size based empirical laws: Adder and Sizer. We assume that any cell size change is a result of equivalent quantity of metabolites produced in proper stoichiometry, and propose that cell divides upon having produced the requisite quantities of the metabolites.

In case of metabolic Adder, whatever be the existing number of metabolites in the cell after birth, the cell needs to produce the new metabolites equal to the threshold parameter. Whereas, in case the Sizer, the cell needs to only produce the difference in quantity between the existing and the threshold (Fig – 1a). We consider that the cell divides only when all the metabolites cross their respective set thresholds, in keeping with a strict requirement of stoichiometry.

We compare the outcome of the generation time distribution when we implement metabolic Adder vs the metabolic Sizer in our model, in Fig – S4a. We found that the distributions obtained for adder and sizer are pretty similar, although they tend to diverge as the number of concurrent cascades (p increases), and also when the substrate import flux (S_{in}) is low.

When we compare the distributions of generation times from sizer and adder after rescaling the distributions with the mean, we can see that adder distributions are narrower with a lower CV (Fig – S4b).

For a single metabolic bottleneck, both laws give identical results (Fig – S4a). However, increase in the number of bottlenecks leads to a deviation between the two models, where, the Adder law consistently yields higher mean generation times. We chose to go ahead with Sizer for all the subsequent simulations, since it is reported that for poor media conditions, i.e. growth on single substrates in minimal media, the observed results suit a sizer better. While the results of growth in rich media, suit an adder better (5).

Lastly, both adder and sizer based simulations result in distributions of generation times that are right skewed and long tailed and fit well by Log GEV distributions (Fig – S4c and S4c).
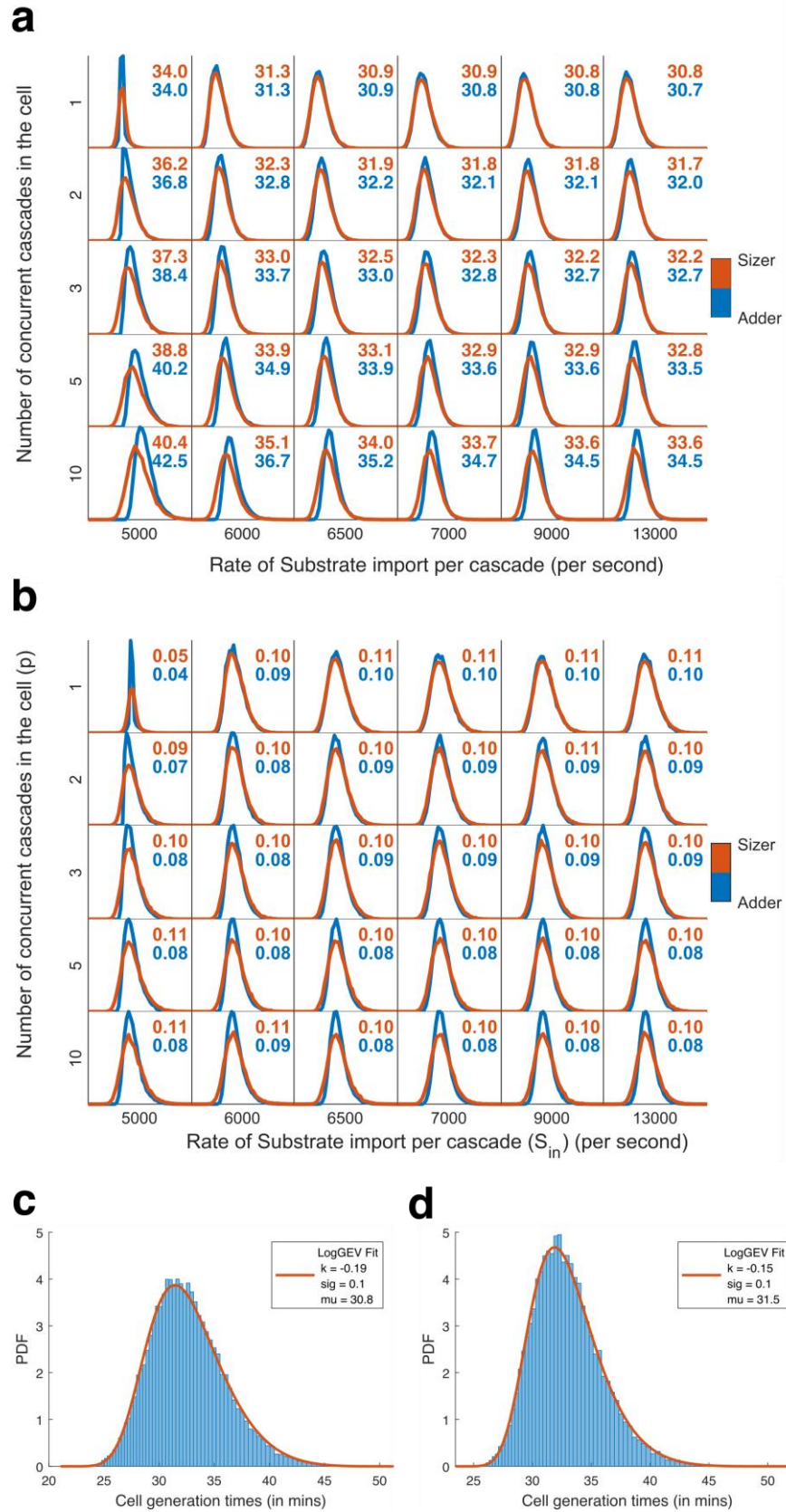
Figure S4: Comparison of Metabolic Adder and Metabolic Sizer Models.
Distributions of generation times from adder and sizer compared, with the mean value (a), rescaled distributions with the CV (b). Fit of the generation time distribution to log-GEV distribution (c) Sizer, (d) Adder.

S5. A simplified steady-state version of reciprocal cross-feeding model

Our model implements the idea of a "metabolic adder" or "metabolic sizer" for cell division, along with a stochastic framework, to reveal the effect of noise on growth outcomes. However, the same model considerations when implemented as a steady state model, cannot distinguish any differences in growth between the different cases.

Take for example, the case of a prototroph, with 3 concurrent limiting metabolites ($p = 3$), each of which is produced by a 3-step linear enzyme pathway ($n = 3$). In contrast to our model with noisy enzyme expression where the enzyme quantity rises, in the steady-state version, we consider a fixed quantity of enzyme present in the cell. The model cell is still fed by a constant import of the substrate (Sin) and cell divides when the threshold requirement of each of the metabolites is met (based on metabolic Sizer). The time duration between successive divisions is noted. Post division the cellular contents are halved and the process repeats.

Upon simulating this steady-state model (scheme shown in Fig – S5b), we obtain a constant generation time by which the metabolite requirements are met. We also see that generation time decreases with increased Substrate import rate (S_{in}), and then saturates (Fig – S5a, Blue line) demonstrating the relationship equivalent to Monod's law.

When a metabolite is directly imported into such a cell, there is no effect on the generation time observed at all (Red line, growth pattern overlaps with the prototroph with no import). This is because, there is no metabolite feedback effects modelled, and thus no metabolite is redistributed to the other pathways, and the cell takes the same amount of time to meet the metabolite requirements for the p pathways (all of which are assumed to be equal).

Upon loss of one pathway (auxotrophy), when the missing metabolite is supplied directly at the required rate (scheme shown in Fig – S5c), lower generation times are observed at lower Substrate import rate (S_{in})(Fig – S5a, Purple), because the available substrate is now utilized by the remaining two pathways instead of three.

If we pair up two such complementary auxotrophs and simulate cross-feeding, the overall time required to meet the cellular demands of all the metabolites will be higher (Fig – S5d) and hence growth will be slower (not shown in Fig – S5a).

However, if we now simulate the case of cross-feeding between auxotrophs, using the idea that the auxotroph now needs to produce double the amount of one of the remaining metabolites for cross-feeding (scheme shown in Fig – S5e), then the advantage observed at low S_{in} is lost, and the growth pattern (Fig – S5a, Yellow) overlaps with the prototroph.

Thus, we show that an equivalent steady state version of our model (without any feedback effects) would not be able to demonstrate any growth impact of (a) metabolite import and (b) metabolite cross-feeding. (a) because there is no feedback modelled, and (b) because there is no metabolite savings when the cell overexpresses the metabolite. In contrast, our model with gene expression noise, yields the distribution of the generation times, due to the variation in enzyme quantity with time. The model is able to show a growth advantage in case of (a) because the biosynthetic pathway of the imported metabolite ceases to be a bottleneck for the cell. In case of (b) during cross-feeding, again it is the reduction in the number of bottlenecks that imparts the growth advantage.
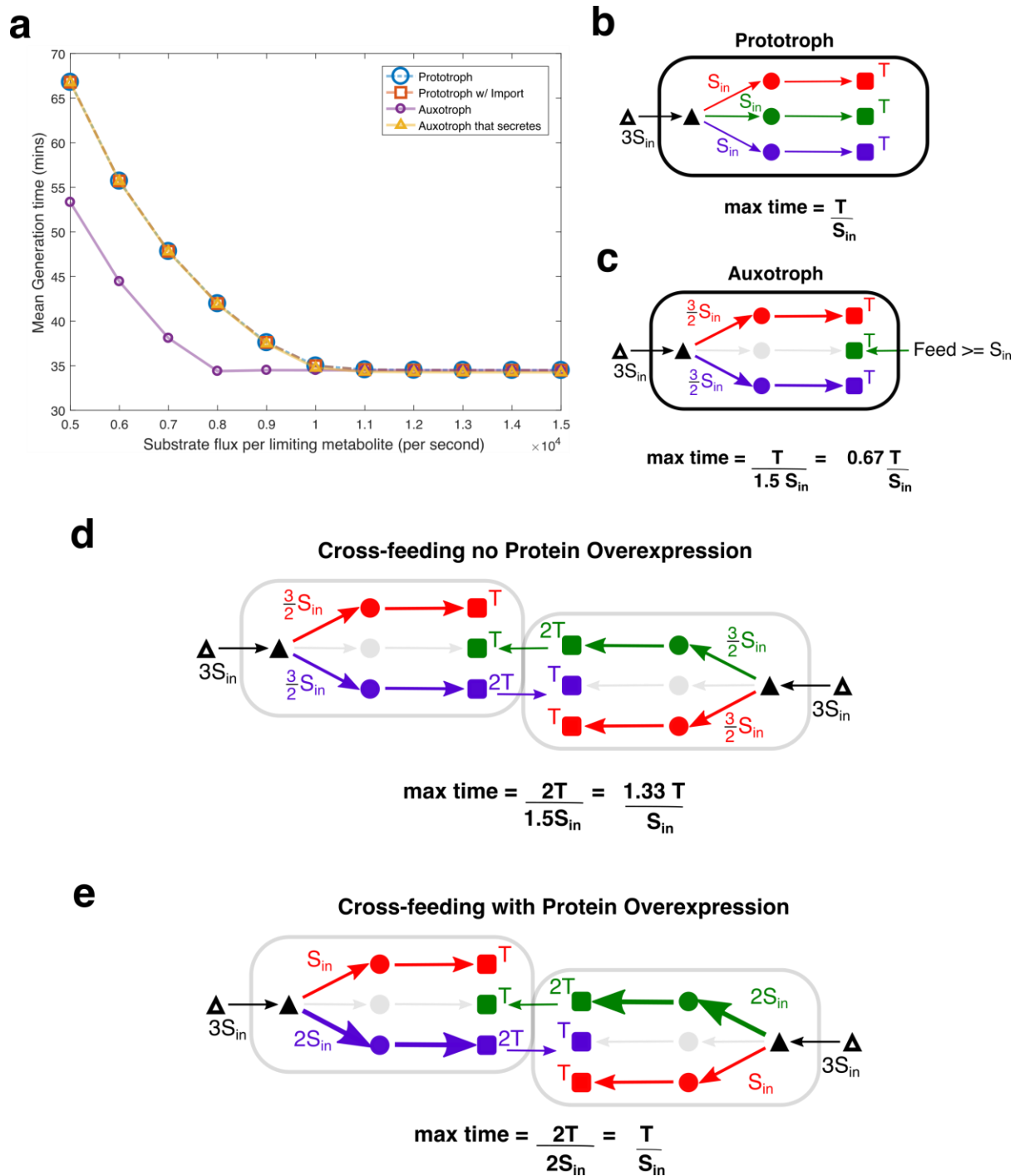
Figure S5: A simplified steady-state version of reciprocal cross-feeding model

(a) Comparing the mean generation time of cells, when considering a steady-state model of prototrophs (blue)(b), prototrophs w/ import (red), auxotrophs (purple)(c) and auxotrophs that overexpress and secrete (yellow)(e).

(b-e) Scheme of the steady-state models for different cases.

S6. Effect of different modelling criteria on the nature of cell generation times observed

Imperfect partition of cells

The only source of stochastic noise we consider in our model is the burst-like gene expression process. However, other sources can also add noise to the cellular growth outcome such as variation in cellular partition ratio, protein translation, and mRNA degradation. Nevertheless, their relative importance varies across different growth rates, with gene transcription and cellular partition being the most important, while mRNA degradation and protein translation are important only at very low rates of growth (6). Hence, we discuss only the effect of imprecise partitioning.

Although the process of cell division in bacteria is highly robust and precise, the two daughter cells obtained are not always of equal sizes. Discrepancies in partition ratio are rare in simple rod-shaped cells, but higher in case of other cell shapes, and on an average, the Coefficient of Variation (CV) in terms of cell length ranges from 3 – 15% (7). Moreover, the profile of noise contribution due to unequal partitioning of the cell has been shown to be virtually indistinguishable compared to stochastic gene transcription (4). We incorporate a randomly sampled partition ratio from a Normal distribution, with mean 0.5 and CV = 0.1, to simulate imperfect division. We observe that the additional noise delays the cell division process, and the distribution of generation times is shifted to the right (Fig – S6).

Effect of gene organisation as Operon

Bacterial genes that are co-expressed are mostly organised as a contiguous unit in the genome called operon (8–13). Our model design thus assumes that all the biosynthetic pathway enzymes occur in the same operon and share the same transcriptional burst profile. If the enzymes were organised separately and transcribed independently, each with its own burst profile, then the noisy lack of synchrony would not only lead to wasted resources (14, 15), we also expect a delay in the metabolite production and hence cell division. Simulating our model with independent expression shows the distribution of generation times is shifted to the right, towards higher values (Fig – S6).

Our model thus demonstrates that operon structure may also lead to kinetic (growth rate) gains for the cell, in addition to the already hypothesised economic gains (14).
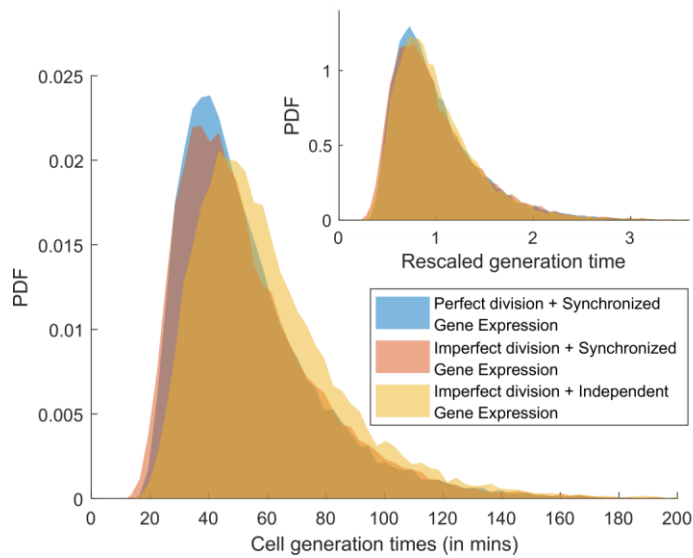
Figure S6: Effect of different modelling criteria on the cell generation time distributions

(Inset) shows the distributions rescaled by mean.

<u>Note</u>: The results shown here use a different set of gene expression and metabolite threshold than in the main paper.

S7. Statistical Test to validate the observed patterns in the data

Here we report the Statistical tests done to show the statistical significance of the patterns we observe. We used Two-way ANOVA to compare the effect of two parameters simultaneously on the growth rate.

For all the tests we use the raw simulated generation times. We have $2^{13} - 1 = 8191$ data points for each independent run, and we performed 3 to 6 independent runs of the simulations. Thus, in each dataset we have at least $8191 \times 3 = 24573$ replicate data points for each combination of the factors.

We used *anova2* function (with balanced test design) in MATLAB, to perform the two-way ANOVA test. Across most conditions, the test results indicate that the null hypothesis that tested groups are equal to each other is rejected with a probability reported as p = 0E0 (i.e. p << 0.0001). However, the test also reports very high interaction between the two parameter groups compared, which is expected since the tested groups are continuous parameter variables and not discrete groups.

Table headers: Sources of variability (Source), Sum of squares due to each source (SS), Degrees of freedom associated with each source (df), Mean squares for each source, which is the ratio SS/df (MS), F-statistic, which is the ratio of the mean squares (F), p-value, which is the probability that the F-statistic can take a value larger than the computed test-statistic value (Prob>F).

Table for Fig – 2d

Source	SS	df	MS	F	Prob>F
Columns	4.65E+06	4.00E+00	1.16E+06	7.89E+04	0.00E+00
Rows	8.70E+08	1.40E+01	6.22E+07	4.22E+06	0.00E+00
Interaction	1.67E+06	5.60E+01	2.98E+04	2.03E+03	0.00E+00
Error	2.71E+07	1.84E+06	1.47E+01		
Total	9.04E+08	1.84E+06			

Table for Fig – 3c

Source	SS	df	MS	F	Prob>F
Columns	3.64E+08	4.00E+00	9.10E+07	2.56E+03	0.00E+00
Rows	1.77E+10	5.00E+00	3.55E+09	9.98E+04	0.00E+00
Interaction	4.78E+07	2.00E+01	2.39E+06	6.72E+01	1.53E-272
Error	6.11E+10	1.72E+06	3.55E+04		
Total	7.93E+10	1.72E+06			

Table for Fig – 3g

Source	SS	df	MS	F	Prob>F
Columns	1.62E+12	5.00E+00	3.23E+11	4.41E+06	0.00E+00
Rows	1.48E+11	5.00E+00	2.95E+10	4.02E+05	0.00E+00
Interaction	2.17E+11	2.50E+01	8.69E+09	1.18E+05	0.00E+00
Error	6.49E+10	8.85E+05	7.34E+04		
Total	2.05E+12	8.85E+05			

Table for Fig – 4b

Compared only the results of simulating auxotroph growth (solid colour lines in Fig – 4b), and neglected feed = 12500, since the growth rate saturates and feed = 7500 and 12500 are identical.

Source	SS	df	MS	F	Prob>F
Columns	1.88E+05	5.00E+00	3.76E+04	2.97E+00	0.011
Rows	5.47E+11	2.00E+00	2.74E+11	2.16E+07	0.000
Interaction	2.55E+05	1.00E+01	2.55E+04	2.01E+00	0.028
Error	7.47E+09	5.90E+05	1.27E+04		
Total	5.55E+11	5.90E+05			

Table for Fig – 5b

Source	SS	df	MS	F	Prob>F
Columns	1.13E+12	2.80E+01	4.03E+10	1.39E+06	0.00E+00
Rows	9.81E+10	4.00E+00	2.45E+10	8.45E+05	0.00E+00
Interaction	4.72E+10	1.12E+02	4.22E+08	1.45E+04	0.00E+00
Error	1.38E+11	4.75E+06	2.90E+04		
Total	1.41E+12	4.75E+06			

Table for Fig – S12a

Source	SS	df	MS	F	Prob>F
Columns	1.74E+08	6.00E+00	2.89E+07	8.11E+02	0.00E+00
Rows	3.60E+09	5.00E+00	7.19E+08	2.02E+04	0.00E+00
Interaction	5.91E+08	3.00E+01	1.97E+07	5.53E+02	0.00E+00
Error	2.45E+10	6.88E+05	3.56E+04		
Total	2.89E+10	6.88E+05			

Table for Fig – S12b

Source	SS	df	MS	F	Prob>F
Columns	2.00E+10	7.00E+00	2.86E+09	7.76E+04	0.00E+00
Rows	4.12E+10	4.00E+00	1.03E+10	2.80E+05	0.00E+00
Interaction	3.75E+09	2.80E+01	1.34E+08	3.64E+03	0.00E+00
Error	4.82E+10	1.31E+06	3.68E+04		
Total	1.13E+11	1.31E+06			

Table for Fig – S12c

Source	SS	df	MS	F	Prob>F
Columns	4.53E+09	4.00E+00	1.13E+09	2.99E+04	0.00E+00
Rows	2.68E+10	4.00E+00	6.69E+09	1.77E+05	0.00E+00
Interaction	1.09E+09	1.60E+01	6.83E+07	1.80E+03	0.00E+00
Error	3.10E+10	8.19E+05	3.79E+04		
Total	6.34E+10	8.19E+05			

Table for Fig – S12d

Source	SS	df	MS	F	Prob>F
Columns	5.01E+09	5.00E+00	1.00E+09	3.58E+04	0.00E+00
Rows	4.66E+09	4.00E+00	1.16E+09	4.16E+04	0.00E+00
Interaction	2.20E+08	2.00E+01	1.10E+07	3.93E+02	0.00E+00
Error	2.75E+10	9.83E+05	2.80E+04		
Total	3.74E+10	9.83E+05			

S8. Comparison of generation time distributions of prototrophs and auxotrophs when growth rates are equal

Here we compare the overlap of the distributions of generation times between cases when the growth rates computed from the generation times are equal. In our simulations we demonstrate that by externally supplying a limiting metabolite, prototrophs can grow faster, same as the prototroph with one less bottleneck. Auxotrophs can also enjoy the same benefit by losing one of the limiting metabolite biosynthetic pathway.

We compare between the generation time distribution of a prototroph with two bottleneck metabolites ($p = 2$), against the following: (a) prototroph ($p = 3$), fed one limiting metabolite at a high rate, (b) auxotroph (originally $p = 3$), fed the missing limiting metabolite at a high rate.
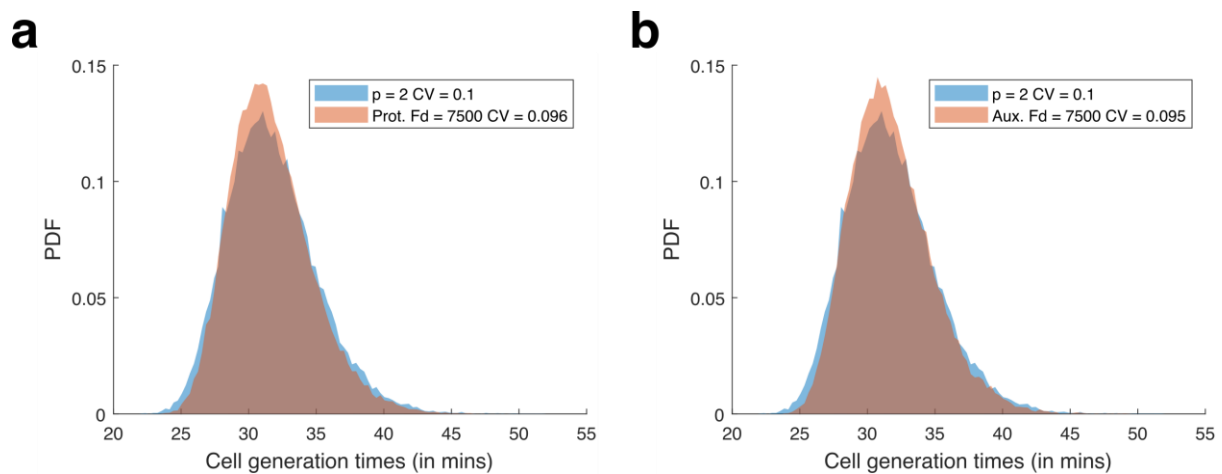
Figure S8: Comparison of generation time distributions of prototroph with lower bottleneck (p = 2) versus (a) prototroph, and (b) auxotroph, when fed the limiting metabolite at 7500/sec such that the growth rates are equal.

S9. List of Parameters

| PARAMETER	VALUE	SOURCE
Mean mRNA lifetime	25 mins	Bionumbers 112326
Mean protein lifetime	20 hours	Bionumbers 111930
Average Enzyme gene length	1029 bp / 343 aa	Bionumbers 108985
Transcription Rate	55 nt/sec	Bionumbers 100059
Translation Rate	20 aa/sec	Bionumbers 100059
Mean duration of a Transcription burst (t_{ON})	4 mins	Optimized (See Supplementary S3)
Mean wait time duration between Transcription bursts (t_{OFF})	2.4 mins	Optimized (See Supplementary S3)
Median enzyme turnover number or catalytic constant (k_{cat})	10 per sec	Bionumbers 111411
Median enzyme half-saturation constant (K_M)	100 µM or 60220 molecules	Bionumbers 111413 (Value converted to molecules assuming a cell volume of $1\mu m^3$)

S10. Metabolic bottlenecks of unequal effect

In a cell, the demand for all metabolites (biomass precursors) is not equal. The cell could however regulate substrate flux distributed to different pathways and the amount of enzyme produced based on the kinetic parameters and the demand, and try to have all the metabolites produced within the shortest time.

Even then some metabolite pathways continue to bottleneck growth more strongly than others. Not only have experiments shown that altering the wildtype gene expression improves growth (16), but Genome Scale Metabolic flux balance models have been successfully used to identify metabolic bottlenecks and optimize the strains (17, 18). Moreover, analysis of lab adapted strains selected for growth has also shown that they improve growth my optimising their flux distribution (19).

Till now our model has only considered the effect of the main bottleneck metabolites (p) on growth. We have neglected the growth effect of other metabolites (q) whose growth effect may be lower due to lower metabolite threshold requirements. Here we consider such a simulation, where both p and q metabolites are modelled. We consider $p = 1$, and $q = 9$, such that $p + q = 10$. In Fig – S10(A), the black and grey dashed lines represent growth of cells with only equal bottlenecks (p) 1 and 10 respectively. We vary the difference between the metabolite thresholds of p and q metabolites in percentages: 2.5, 10, 25, and 50.

We find that when the difference is high, the cell acts as if it has only the p bottlenecks limiting growth. However, as the differences reduce, growth reduces and cell acts similar to one with higher p.
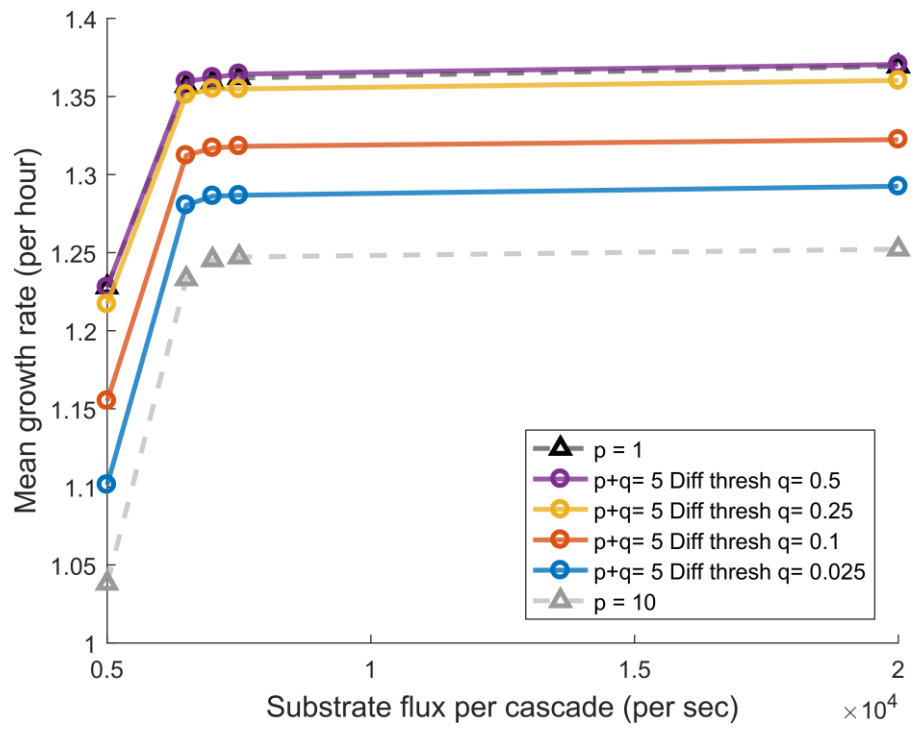
Figure S10: Comparison of growth rates between cells with only equal bottlenecks (only p) versus those with unequal bottlenecks (p and q).

S11. Upstream Catabolism as a noisy process

The carbon substrate the cell uptakes is broken down by catabolic pathways and channelled to various anabolic pathways to produce the necessary biomass precursors. For modelling convenience, we chose the substrate supply rate from catabolism as a constant in our model.

Here we discuss the consequences of modelling the common substrate supply as a noisy process. For this we consider an additional enzymatic step before the anabolic pathways, which has a kinetic constant p times the kinetic constant of the anabolic enzymes.

We compare this modified model, with one catabolic enzyme step and two anabolic enzyme steps ($n = 2$) with the original model with three anabolic enzyme steps pathway ($n = 3$). The resultant distributions are close and comparable, but not exact. The growth rate estimated from the distributions show that including noisy catabolism reduces the maximum growth rate. Hence, even if we consider a model with "noisy catabolism", we do not expect the results derived from our model to change qualitatively.
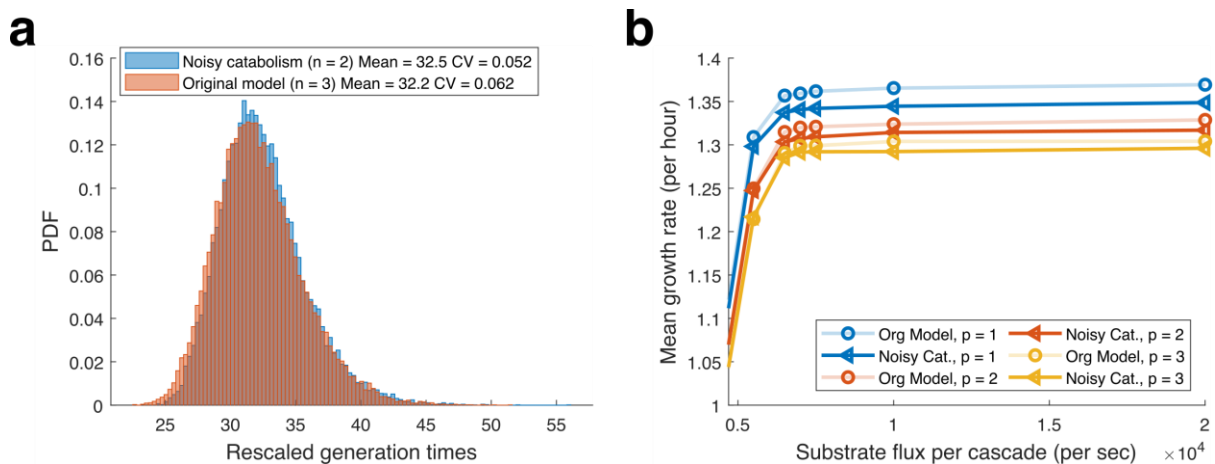
Fig – S11: Comparison of effect of modelling substrate supply as a noisy process.
Generation times are slightly higher for noisy catabolism (a) and corresponding growth rates estimated are also lower compared to the constant substrate flow case (b).

S12. Effect of feedback regulation on metabolite biosynthesis and the effect of noisy metabolite import

Effect of feedback regulation

When the metabolites synthesised in the cell are available in the environment, cells readily import them into the cell, inhibiting the internal biosynthesis due to feedback regulation. The substrate flux utilised by the pathway is reduced, and more substrate flux is available for use by the other competing biosynthesis pathways. Till now, in our simulations, we have neglected this effect. Here we implement the inhibition due to feedback regulation into our model by incorporating a scaling parameter multiplied with the enzyme's catalytic constant, which reduces the effective flux through the pathway, making the metabolite imported directly. Thus, the competing biosynthetic pathways can utilise the excess substrate flux to produce other limiting metabolites.

By varying the scaling parameter, we vary the amount of feedback as a percentage reduction in the enzyme's catalytic constant. We also vary the rate of metabolite import (Feed) into the cell and the substrate flux (S_{in}) as done before (Results Section 3: Effect of metabolite uptake and secretion on simulated cells). At low metabolite import rates, increasing feedback strength leads to a decrease in the growth rate since the metabolite production rate slows down (Fig – S12a). At high metabolite import rates, we find that increasing feedback strength makes more substrate flux available to the competing biosynthetic pathways, and hence the growth rate increases in low substrate flux (S_{in}) cases (Fig – S12b). No further increase in growth rate is possible at higher substrate flux because the enzyme is limiting.

Effect of noisy metabolite import

In our model, we assume that biosynthetic enzyme gene transcription is a stochastic burst-like process. However, this is true for all genes transcribed in the cell. Thus, the number of transporter proteins in the cell should also vary. Nevertheless, in our simulations, we assumed that metabolite import at a constant rate for the sake of simplicity.

Here, we explore how our observations may change when we model metabolite transport as a noisy process. We assume that the transporter protein's expression parameters are the same as the biosynthetic enzymes for ease of comparison due to identical noise characteristics. We also assume the same catalytic constant for the transporter as the enzyme. However, we use a scaling parameter (Feed ratio) multiplied by the catalytic constant to vary the rate of import.

We have shown that importing one of the limiting metabolites into the cell at a sufficiently high rate allows prototrophic cells to enjoy a growth advantage (Fig – 3c). We have also demonstrated that auxotrophs require a sufficiently high supply of the metabolite they cannot produce to enjoy a growth advantage (Fig – 4b). In the case of auxotrophs and cross-feeders, one may intuit that if the growth advantage is a consequence of reduced noise, then incorporating noise in transport may cause the observed growth advantage to disappear. We thus incorporate noise into the process of transport and then simulate their growth, as done before in Results Section 4 and 5.

Upon simulating the growth of auxotrophs with noisy metabolite import, we see that the growth advantage observed sustains, even when the import and biosynthesis have the same catalytic constant (Feed ratio = 1, Fig – S12b).

In the case of cross-feeding, where we study the growth of a metabolite overexpressing and secreting auxotroph as a proxy, we again observe that the growth advantage sustains with noisy metabolite import (Fig – S12c).

It is important to note that when comparing the noise due to biosynthesis versus transport, biosynthesis involves multiple steps, while transport is always a one-step process. Our model considers that each biosynthetic pathway is linear and composed of n enzyme steps. Through this work, we have assumed 3 enzyme steps ($n = 3$). In Fig – S12d, we plot the growth rate of cells against the rate of substrate import and vary the number of enzyme steps (n). We observe that the growth rate decreases as the number of enzyme steps (n) increase. Thus, even when transport is modelled as a stochastic process, the growth advantage sustains due to the difference in the number of linear steps between the two processes.
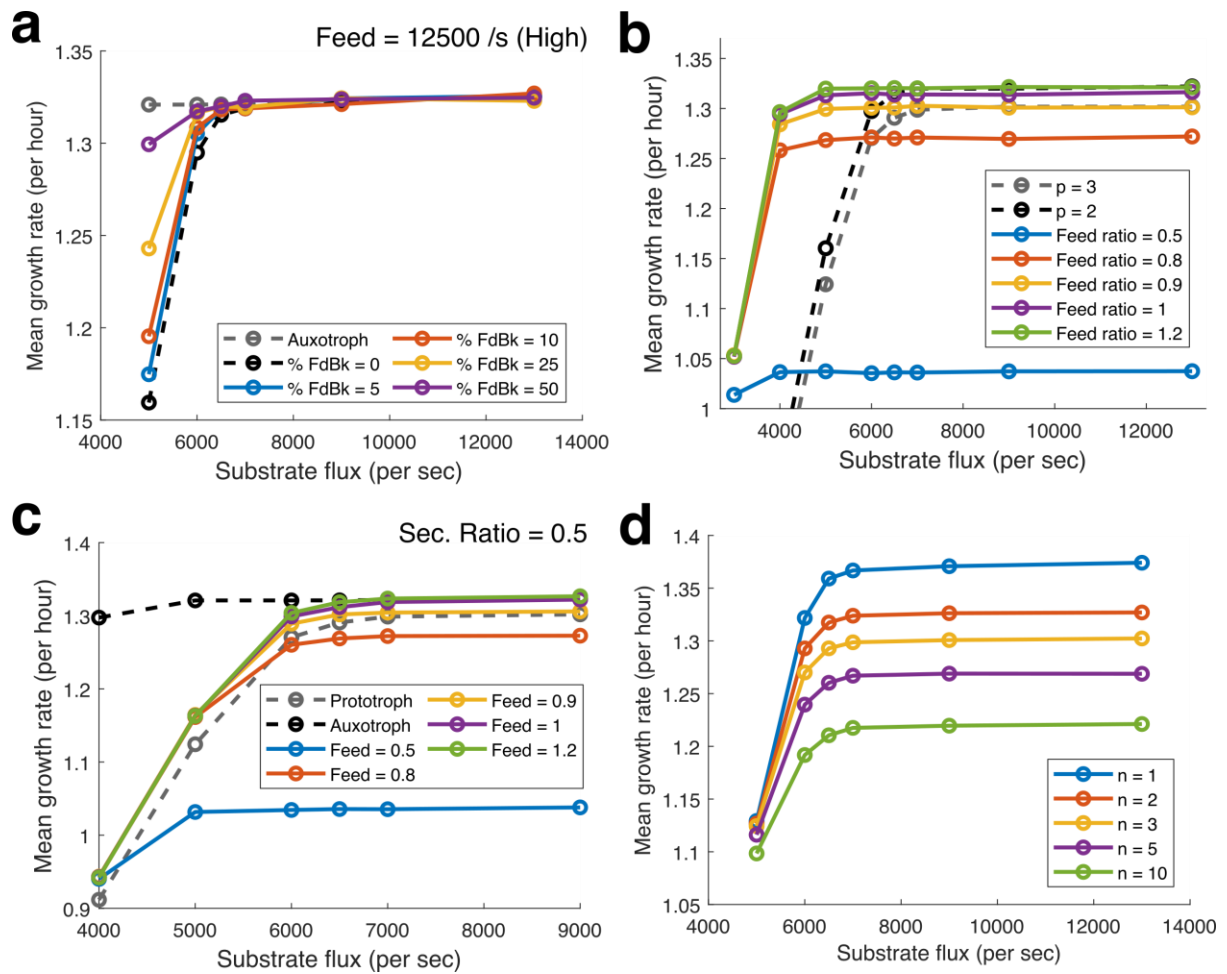
Figure S12: Effect of feedback on metabolite biosynthesis and noise during metabolite import

(a) **Effect of feedback on metabolite biosynthesis**
Comparison of the mean growth rate of the simulated prototroph versus different rates of substrate import flux (S_{in}), when fed a limiting metabolite at a high rate = 12500/s, with varying strengths of feedback regulation (%). Growth rate of prototroph with no feedback effects (black dotted line) and auxotroph (grey dotted line).

(b-c) **Effect of noise during metabolite import**
Comparison of the mean growth rate versus different rates of substrate import flux (S_{in}), for (c) auxotrophs, and (d) auxotrophs that overexpress and secrete a limiting metabolite (proxy for cross-feeders). In (c) the grey and black dotted lines represent the prototrophs with $p = 3$ and $p = 2$ bottleneck metabolites respectively. In (d) the grey and black dotted lines represent the growth profile of corresponding prototroph and auxotroph.

(d) **Effect of varying the number of enzyme steps in the biosynthetic pathway**
Comparison of the mean growth rate versus different rates of substrate import flux (S_{in}), for a prototroph with 3 limiting metabolites ($p = 3$), while varying the number of enzyme steps in the biosynthetic pathways (n).

Supplementary References

1.   Taheri-Araghi S, Bradde S, Sauls JT, Hill NS, Levin PA, Paulsson J, Vergassola M, Jun S. 2015. Cell-Size Control and Homeostasis in Bacteria. Curr Biol 25:385–391.

2.   Pugatch R. 2015. Greedy scheduling of cellular self-replication leads to optimal doubling times with a log-Frechet distribution. Proc Natl Acad Sci 112:2611–2616.

3.   Golding I, Paulsson J, Zawilski SM, Cox EC. 2005. Real-time kinetics of gene activity in individual bacteria. Cell 123:1025–1036.

4.   Huh D, Paulsson J. 2011. Non-genetic heterogeneity from stochastic partitioning at cell division. Nat Genet 43:95–100.

5.   Wallden M, Fange D, Lundius EG, Baltekin Ö, Elf J. 2016. The Synchronization of Replication and Division Cycles in Individual E. coli Cells. Cell 166:729–739.

6.   Thomas P, Terradot G, Danos V, Weiße AY. 2018. Sources, propagation and consequences of stochasticity in cellular growth. Nat Commun 9:4528.

7.   Trueba FJ. 1982. On the precision and accuracy achieved by Escherichia coli cells at fission about their middle. Arch Microbiol 131:55–59.

8.   Jacob F, Monod J. 1961. Genetic regulatory mechanisms in the synthesis of proteins. J Mol Biol 3:318–356.

9.   Zheng Y, Szustakowski JD, Fortnow L, Roberts RJ, Kasif S. 2002. Computational Identification of Operons in Microbial Genomes. Genome Res 12:1221–1230.

10.   Price MN, Arkin AP, Alm EJ. 2006. The Life-Cycle of Operons. PLoS Genet 2:e96.

11.   Price MN, Huang KH, Arkin AP, Alm EJ. 2005. Operon formation is driven by co-regulation and not by horizontal gene transfer. Genome Res 15:809–819.

12.   Rocha EPC. 2008. The Organization of the Bacterial Genome. Annu Rev Genet 42:211–233.

13.   Sabatti C, Rohlin L, Oh M-K, Liao JC. 2002. Co-expression pattern from DNA microarray experiments as a tool for operon prediction. Nucleic Acids Res

30:2886–2893.

14.   Sneppen K, Pedersen S, Krishna S, Dodd I, Semsey S. 2010. Economy of Operon Formation: Cotranscription Minimizes Shortfall in Protein Complexes. MBio 1.

15.   Ray JCJ, Igoshin OA. 2012. Interplay of Gene Expression Noise and Ultrasensitive Dynamics Affects Bacterial Operon Organization. PLoS Comput Biol 8:e1002672.

16.   Keren L, Hausser J, Lotan-Pompan M, Vainberg Slutskin I, Alisar H, Kaminski S, Weinberger A, Alon U, Milo R, Segal E. 2016. Massively Parallel Interrogation of the Effects of Gene Expression Levels on Fitness. Cell 166:1282-1294.e18.

17.   Kim B, Kim WJ, Kim DI, Lee SY. 2015. Applications of genome-scale metabolic network model in metabolic engineering. J Ind Microbiol Biotechnol 42:339–348.

18.   Maia P, Rocha M, Rocha I. 2016. In Silico Constraint-Based Strain Optimization Methods: the Quest for Optimal Cell Factories. Microbiol Mol Biol Rev 80:45–67.

19.   Lewis NE, Hixson KK, Conrad TM, Lerman JA, Charusanti P, Polpitiya AD, Adkins JN, Schramm G, Purvine SO, Lopez-Ferrer D, Weitz KK, Eils R, König R, Smith RD, Palsson BØ. 2010. Omic data from evolved E. coli are consistent with computed optimal growth from genome-scale models. Mol Syst Biol 6:390.